ECN

Energy research Centre of the Netherlands

Carbon Capture by Sorption-Enhanced Water-Gas Shift Reaction Process using Hydrotalcite-Based Material

E.R. van Selow

P.D. Cobden

P.A. Verbraeken

J.R. Hutfton

R.W. van den Brink

Published in the Industrial & Engineering Chemistry Research, 2009 pp 4184 - 4193

ECN-W-09-045 December 2009

Article

Carbon Capture by Sorption-Enhanced Water#Gas Shift Reaction Process using Hydrotalcite-Based Material

E. R. van Selow, P. D. Cobden, P. A. Verbraeken, J. R. Hufton, and R. W. van den Brink

Ind. Eng. Chem. Res., **Article ASAP** • DOI: 10.1021/ie801713a • Publication Date (Web): 08 April 2009

Carbon Capture by Sorption-Enhanced Water−Gas Shift Reaction Process using Hydrotalcite-Based Material

E. R. van Selow,*,† P. D. Cobden,† P. A. Verbraeken,† J. R. Hufton,‡ and R. W. van den Brink†

Energy Research Centre of The Netherlands, P.O. Box 1, 1755 ZG Petten, The Netherlands, and Air Products and Chemicals, Inc., 7201 Hamilton Boulevard, Allentown, Pennsylvania

A novel route for precombustion decarbonization is the sorption-enhanced water−gas shift (SEWGS) process. In this process carbon dioxide is removed from a synthesis gas at elevated temperature by adsorption. Simultaneously, carbon monoxide is converted to carbon dioxide by the water−gas shift reaction. The periodic adsorption and desorption of carbon dioxide is induced by a pressure swing cycle, and the cyclic capacity can be amplified by purging with steam. From previous studies is it known that for SEWGS applications, hydrotalcite-based materials are particularly attractive as sorbent, and commercial high-temperature shift catalysts can be used for the conversion of carbon monoxide. Tablets of a potassium promoted hydrotalcite-based material are characterized in both breakthrough and cyclic experiments in a 2 m tall fixed-bed reactor. When exposed to a mixture of carbon dioxide, steam, and nitrogen at 400 °C, the material shows a breakthrough capacity of 1.4 mmol/g. The sharp adsorption front is accompanied by an exotherm that travels along the bed. Even after breakthrough carbon dioxide continues to be taken up by the bed albeit at a much lower rate. It is shown that the total capacity of this material can exceed 10 mmol/g, which has not been reported before. Desorption curves indicate efficiencies of removing additional carbon dioxide by purging with low-pressure, superheated steam at various flow rates. During cyclic operation for more than 1400 adsorption and desorption cycles, the carbon dioxide slip is very low and remains stable which indicates that carbon recoveries well above 90% can be obtained. The sorbent shows a stable cyclic capacity of 0.66 mmol/g. In subsequent experiments the material was mixed with tablets of promoted iron−chromium shift catalyst and exposed to a mixture of carbon dioxide, carbon monoxide, steam, hydrogen, and nitrogen. It is demonstrated that carbon monoxide conversion can be enhanced to 100% in the presence of a carbon dioxide sorbent. At breakthrough, carbon monoxide and carbon dioxide simultaneously appear at the end of the bed. During more than 300 cycles of adsorption/reaction and desorption, the capture rate, and carbon monoxide conversion are confirmed to be stable. Two different cycle types are investigated: one cycle with a CO_2 rinse step and one cycle with a steam rinse step. The performance of both SEWGS cycles are discussed. These experimental results will allow optimization of process conditions and cycle parameters, and especially the reduction of steam consumption needed for sorbent regeneration. The results will provide the basis for scale-up to a pilot unit, which will demonstrate precombustion decarbonization in fossil-fuels-based power generation or hydrogen production.

1. Introduction

Global atmospheric concentration of CO_2 has increased by more than 35% since the beginning of the industrial revolution around 1750.[1] The global increase in CO_2 concentration is primarily related to the use of fossil fuels and land-use changes. Multiple independent lines of evidence point to anthropogenic emissions being the major cause of global warming. With current mitigation policies in place, greenhouse gas emission will continue to grow and contribute to global warming in the near future.[2] In the energy supply sector, carbon capture and sequestration (CCS) needs commercialization before 2030 to help meet mitigation goals.

This paper discusses bench-scale results of a precombustion decarbonization technology for CCS called sorption-enhanced water−gas shift (SEWGS). SEWGS combines a high-temperature CO_2 sorbent and a high-temperature shift catalyst to produce hot and separated H_2 and CO_2 product streams from syngas.[3−5] The sorbent is periodically regenerated, and the process comprises multiple reactors which are operated in cycles, resembling cycles of a pressure swing adsorption (PSA) process. The H_2 can be used in a combined cycle power plant to produce electricity, and the CO_2 is prepared for sequestration. A major advantage of SEWGS is higher efficiency brought about by the separation of CO_2 and H_2 at high temperature (400 °C). Most other precombustion decarbonization technologies require much lower temperatures for CO_2 removal, which means steam in the raw syngas is lost by condensation and the H_2 needs to be reheated before it can enter the gas turbine. Steam is used in both the adsorption-reaction step and in the desorption step of the cyclic process. In the latter it acts as a condensable component in the reactor purge stream that is easily removed to leave a relatively pure CO_2 stream suitable for sequestration. A major challenge for SEWGS optimization is reducing the process steam requirements and subsequently boosting the electrical efficiency of the overall power generation process.[6]

Several materials are known to capture CO_2 at 400 °C in the presence of steam.[7,8] Much attention has been given to potassium promoted hydrotalcite-based materials.[3−23] We consider these materials to be particularly well suited for application in the SEWGS process. There is still some discussion in the literature as to the mechanism and description of the interaction of CO_2 with potassium-promoted hydrotalcite-based materials.[21] In addition to the relatively simple Langmuir description,[10]

* To whom correspondence should be addressed. E-mail: vanselow@ecn.nl. Tel.: +31 224 564116. Fax +31 224 568489.
† Energy Research Centre of The Netherlands.
‡ Air Products and Chemicals, Inc.

10.1021/ie801713a CCC: $40.75

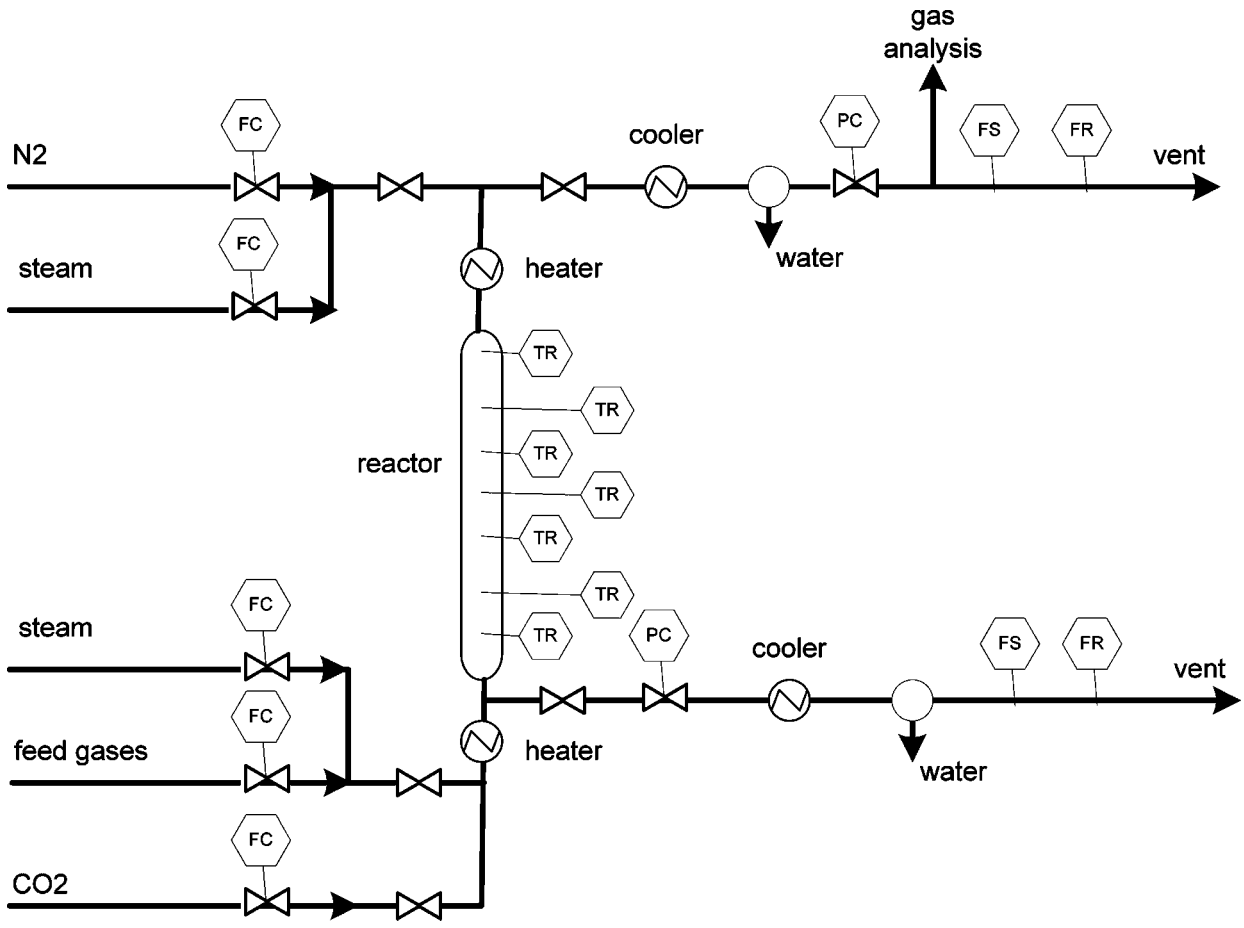

Figure 1. Test rig flow scheme.

nonequilibrium coupled reactions,[16,17] CO_2 complexation reactions,[18] and coupled exothermic−endothermic reactions[21] have been suggested. Recently it was reported that the main interaction of CO_2 with such materials at the relevant temperature was due to an aluminum−potassium-carbonate species, although subject to modification by the presence of magnesium.[22]

Many studies have looked at CO_2 adsorption on hydrotalcites in the presence of steam. In terms of capacity, performance is generally seen to improve in the presence of steam. However, until now, even though this phenomenon has been seen in multiple experimental studies, there has been little effort to explain it. On the side of modeling studies, only a few publications exist which discuss how this would affect system performance. On the side of experimental studies, systematic measurements on the size of this effect as a function of CO_2 and H_2O concentration and pressure have yet to appear. The effect of steam on CO_2 uptake was taken into account by Ding and Alpay.[10] A predictive model was obtained by assigning different CO_2 Langmuir isotherm parameters for wet and dry conditions. The isotherm parameters were derived from experiments described in a previous publication.[11] Ebner et al. [16] included H_2O in a model based on a system of nonequilibrium coupled reactions, but it has not been used yet to study the effect of H_2O on CO_2 uptake. Moreover, experiments have rarely been reported in which hydrotalcites have been exposed to high-pressure steam. Anand et al.[24] concluded that steam improved capacity, but even after exposure to 10 bar steam and 0.3 bar CO_2 for tens of days, no extra capacity above 0.6 mmol/g was observed. In spite of that, up to 8.3 mmol/g CO_2 has been recovered from these compounds after use for up to a week under industrial-like conditions.[5] Only the nonequilibrium coupled reactions model currently could come close to describing this high adsorption capacity.[16,17] This paper will show that remarkably even higher loadings of CO_2 can be achieved when both steam and CO_2 concentrations are in the range envisioned for industrial operation.

SEWGS process cycles including either a CO_2 rinse or a steam rinse step have been proposed for efficiently recovering CO_2 from syngas.[4,9] Addition of a rinse step maximizes the H_2 recovery. Other cycles with this class of material have also been proposed for postcombustion capture.[25,26] This paper shows a comparison of two SEWGS cycles applied to a single reactor vessel, one cycle with a CO_2 rinse step and one with a steam-rinse step.

2. Experimental Details

2.1. Setup. Calcined pellets of K_2CO_3-promoted hydrotalcite-based material, designated as PURALOX MG70, were obtained from SASOL Germany (bulk density 390 kg/m^3, diameter 4.8 mm). High-temperature shift catalyst pellets, FeCr based, with size similar to the size of the sorbent pellets, were obtained from a commercial manufacturer. Experiments were carried out in a 2 m tall column with an internal diameter of 38 mm. The reactor wall was kept at 400 °C by electric heating and insulation. Thermocouples were used to monitor the bed temperatures at seven equally spaced axial positions of the reactor. Figure 1 shows a flow scheme of the test rig. Feed gases were obtained from gas cylinders: H_2 and CO from Air Liquide, CO_2 and N_2 from Linde. Deionized water was used to generate 40 bar steam in a boiler. Pure gases and superheated steam were mixed in desired quantities in order to obtain the desired feed

gas composition and flow rate. Bronkhorst thermal mass flow controllers were used for H_2, CO, and N_2, and Bronkhorst coriolis-type mass flow sensors were used for CO_2 and steam. Feed gases were heated to 400 °C in electric heaters. Product gases were cooled down to 5 °C and condensate was removed in knockout drums. Integrated quantities of dry product gases at standard state conditions (0 °C, 1 atm) were calculated from measurements of actual gas quantities by Ritter bellows-type volumetric dry gas meters and correcting for the slight deviations from standard pressure and temperature using the ideal gas law. Instantaneous flow rates of effluent gases were measured by Brooks thermal mass flow sensors which were originally calibrated for air, and were corrected for gas composition according to the *k*-values provided by the vendor. Gas analysis was by an Ametek ProLine process mass spectrometer during the sorbent-only experiments, and by an ABB Advance Optima nondispersive IR during sorbent-catalyst experiments.

2.2. Experimental Procedures and Test Conditions. Three types of experiments were performed: breakthrough experiments, desorption experiments, and cyclic experiments. In a first series of experiments, only the sorbent characteristics were investigated, and in a second series the characteristics of a sorbent-catalyst admixture were investigated.

For the first series of experiments, the reactor was fully loaded with 1025 g of sorbent material. The reactor was brought to the operating temperature of 400 °C in a flow of N_2 at a rate of 30 °C/h, and kept at 400 °C for subsequent experiments. The sorbent was exposed to a few thermal cycles from ambient to 400 °C during these experiments due to both scheduled and emergency shutdowns. These thermal cycles did not noticeably affect the performance of the system. Breakthrough experiments were run by feeding the desired feed gas to the reactor at 26−28 bar while continuously monitoring the effluent gas flow rate and composition. Eventually, the sorbent became saturated and CO_2 appeared in the effluent gas (breakthrough). The experiment was continued well beyond breakthrough.

Desorption experiments were conducted to determine how effectively the sorbent could be regenerated. The sorbent was first saturated by feeding with CO_2 and steam at 28 bar and 400 °C. This was followed by a cocurrent rinse of the reactor with high-pressure steam—equivalent to one reactor void volume—and a countercurrent depressurization of the reactor to essentially atmospheric pressure. The bed was then purged with low-pressure steam, and the effluent gas flow rate and composition were monitored. The steam purge was continued until the dry gas flow rate, that is, CO_2, at the reactor outlet was essentially zero.

Cyclic adsorption−desorption experiments were carried out to investigate the stability of the sorbent under cyclic conditions. Feed gas consisted of CO_2, N_2, and steam at 26−28 bar and total flow of 8−12 slpm. The gas composition and cycle parameters are shown in Table 1. A cycle consists of several steps in a fixed order and with a fixed duration. The consecutive steps are (1) feed, during which adsorption (and possibly shift reaction) occur; (2) rinse, for pushing out the gas that is present in the voids; (3) depressurization; (4) purge, for regeneration of the sorbent; (5) repressurization.

The feed and rinse steps take place at high pressure, whereas the purge step takes place at low pressure. The rinse step maximizes the H_2 recovery, which is important for maximizing the plant efficiency and for minimizing the quantity of H_2 in the CO_2 product.

In the second set of experiments the reactor was loaded with an admixture of 891 g of sorbent and 434 g of catalyst pellets, which corresponds with a volume ratio of sorbent to catalyst of 5. The catalyst was reduced in situ according to a standard reduction procedure based on supplier guidelines. The reactor was brought to the operating temperature of 400 °C in a flow of N_2 at a rate of 30 °C/h. Cyclic experiments were carried out to investigate the stability of the sorbent and catalyst during SEWGS conditions and to demonstrate the feasibility of the sorption-enhanced process itself. The feed gas consisted of CO_2, N_2, CO, H_2, and steam. The feed pressure was 26−28 bar and the total flow rate was 7−12 slpm. In both sets of cyclic experiments, the cycle times were chosen such that a small amount of CO_2 was present in the reactor effluent exiting the top of the reactor. These conditions are representative for an envisaged industrial operation. Reactor wall temperature and gas feeding temperature were always kept at 400 °C. In the second set of experiments, a small amount of H_2, typically 0.5 slpm, was added to the purge steam to make sure that the catalyst remained in its reduced state.

The reactor was purged with N_2 for at least 12 h between experiments. The adsorption−desorption cycle parameters are given in Table 1.

Table 1. Cycle Parameters

	cycle 1	cycle 2	cycle 3	cycle 4
Feed				
relative duration (%)	36	44	39	39
CO_2 (%)	12	16	12	12
H_2O (%)	48	49	21	21
N_2 (%)	39	35	36	36
H_2 (%)	0	0	30	30
CO (%)	0	0	1.6	1.6
pressure (bar)	28	28	28	28
Rinse				
relative duration (%)	16	11	13	13
flow direction	cocurrent	countercurrent	cocurrent	countercurrent
composition	CO_2	H_2O	CO_2	H_2O
CO_2-to-C in feed (mol/mol)	2.0	n.a.	1.8	n.a.
steam-to-C in feed (mol/mol)	n.a.	1.9	n.a.	2.3
Depressurization				
relative duration (%)	11	11	13	13
flow direction	countercurrent	countercurrent	countercurrent	countercurrent
end pressure (bar)	2	1	1	1
Purge				
relative duration (%)	9	11	13	13
flow direction	countercurrent	countercurrent	countercurrent	countercurrent
H_2O (%)	73	100	100	100
N_2 (%)	27	0	0	0
pressure (bar)	2	1	1	1
steam-to-CO_2 (mol/mol)	2.2	2.5	2.5	2.3
Repressurization				
relative duration (%)	27	21	19	19
flow direction	countercurrent	countercurrent	countercurrent	countercurrent
H_2O (%)	43	57	55	55
N_2 (%)	57	43	45	45

2.3. Definitions and Calculation Methods. All variables are on a dry basis unless stated otherwise. Stoichiometric breakthrough time t_b is defined as the time when the CO_2 mole fraction of the effluent gas flow is equal to half the mole fraction of the feed. The breakthrough capacity n_b (mmol/g) is defined as

$$n_b = \frac{(t_b F_f - N_{dry}) y_{CO_2,f}}{M} \quad (1)$$

where F_f is the total feed gas flow rate (mol/s), N_{dry} is the moles of gas in the reactor void volume at the reactor pressure and temperature, $y_{CO_2,f}$ is the CO_2 mole fraction in the feed. M is the total mass of sorbent loaded in the reactor after it has been exposed to 400 °C in an ex-situ activation procedure (kg). Adsorption rates are calculated as the difference between the molar CO_2 feed rate and the molar CO_2 effluent rate. Since after breakthrough this difference becomes small, nitrogen is used in the calculations as an inert standard. Total sorption capacities n^* are established by integrating the standard dry volume of gas exiting the reactor during a desorption experiment and subtracting the amount of non-CO_2 void gas attributable to the void space.

The average CO_2 concentration in the top product gas $\bar{y}_{CO_2,t}$ is calculated by dividing the amount of CO_2 leaving the reactor during the feed step by the total amount of dry product gas generated during the feed step subtracted by the amount of dry gas that was present in the reactor at the time the feed step was started:

$$\bar{y}_{CO_2,t} = \frac{\int y_{CO_2,t} F_t \, dt}{\int F_t \, dt - N_{dry}} \quad (2)$$

where F_t is the dry product gas flow rate exiting the top of the reactor (mol/s), N_{dry} is the number of moles of nonadsorbing dry gas needed to pressurize the reactor to feed pressure, and $y_{CO_2,t}$ is the dry CO_2 mole fraction in the effluent stream.

Conversion X for carbon monoxide is calculated from

$$X = 1 - \frac{y_{CO,t} F_t}{F_{CO,f}} \quad (3)$$

where $F_{CO,f}$ is the molar feed flow rate of CO (mol/s).

The effective working capacity n_c (mmol/g) is defined as the quantity of the CO_2 rejected via the depressurization and purge steps during one cycle divided by the total sorbent mass in the reactor:

$$n_c = \frac{\int F_b y_{CO_2,b} \, dt - N_{rinse}}{M} \quad (4)$$

where F_b is the dry effluent flow rate at the reactor bottom during the depressurization or purge steps, $y_{CO_2,b}$ is the CO_2 mole fraction in the reactor effluent at the reactor bottom during the depressurization or purge steps, N_{rinse} is the moles of CO_2 fed during the rinse step, M is the total mass of sorbent loaded in the reactor, and the integration is over the depressurization and purge steps in a cycle. Since the sorption is reversible, the cyclic capacity may be approximated by the following equation, provided that the CO_2 slip in the top product is very low and CO conversion is nearly complete:

$$n_c \approx \frac{\int (F_{CO_2,f} + F_{CO,f}) \, dt}{M} \quad (5)$$

where the CO_2 feed flow rate $F_{CO_2,f}$ and CO feed flow rate $F_{CO,f}$ are integrated over the feed step. Under the applied experimental conditions, the effective working capacity is typically 0.1 mmol/g higher than the cyclic adsorption capacity, since it contains the CO_2 in the void gas as well.

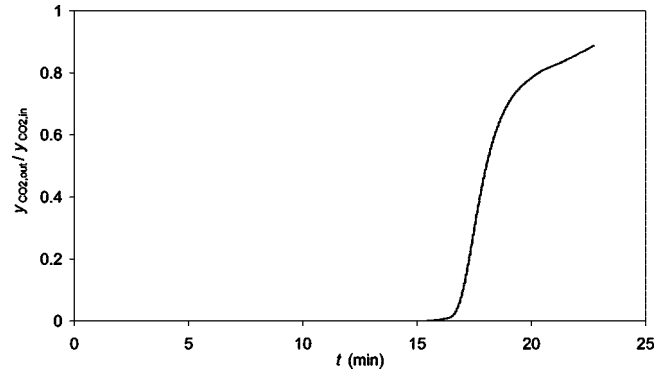

Figure 2. Breakthrough curve for an experiment conducted at a temperature of 400 °C and a pressure of 28 bar. Feed was 2 slpm CO_2 and 7 slpm N_2.

3. Results and Discussion

A first series of experiments was conducted with the reactor loaded with sorbent pellets only in order to investigate important sorbent properties such as CO_2 sorption capacity, stability under conditions of prolonged adsorption−desorption cycles, and the effect of purge flow rate on the regeneration efficiency. For a second series of experiments the reactor was loaded with a mixture of sorbent and catalyst tablets, and the enhancement of the shift reaction by sorption was studied.

3.1. Sorption Only Experiments. Breakthrough and Regeneration Experiments. CO_2 breakthrough experiments were conducted under realistic conditions to determine the breakthrough capacity and sharpness of the adsorption front. Figure 2 shows the effluent gas CO_2 mole fraction when feeding a mixture of CO_2 and N_2 at 400 °C and 28 bar to a bed of fresh sorbent. Breakthrough occurs 16 min after starting the feed. The breakthrough capacity evaluated by eq 1 is 1.4 mmol/g. After breakthrough, the material still takes up CO_2, although at a lower rate than before breakthrough. Breakthrough curves with similar shapes have been previously reported, for instance, by Allam et al.[5] and Lee et al.[18,19]

[18,19]Similar to these studies it is observed that the tail of the breakthrough curve deviates from the theoretical S-shape. This deviation is generally attributed to heat effects.

The reactor contains seven thermocouples in the fixed bed at equidistant intervals of 30 cm. These thermocouples register the exotherms associated with the adsorption reaction. As can be seen from Figure 3, the sharp adsorption front is accompanied by an exotherm that travels along the bed. Observed temperature excursions are on average 42 °C. When the adsorption front has passed, the temperatures fall gradually toward their initial values. The CO_2 adsorption front passes the last thermocouple 14 min after the start of the experiment, just before breakthrough of CO_2 occurs.

The velocity of the thermal front is constant as can be seen from Figure 4. The seven equidistant thermocouples show their respective maximum temperatures at equal time intervals. From this figure it follows that the wave velocity is 0.27 cm/s.

After breakthrough, the effluent CO_2 mole fraction increases but does not attain the CO_2 level of the feed. Hence, the bed continues to take up CO_2 albeit at a lower rate than before breakthrough. To further investigate this phenomenon, we conducted an extended sorption experiment with a feed composed of 20% CO_2, 40% steam, balance N_2, following a cleaning

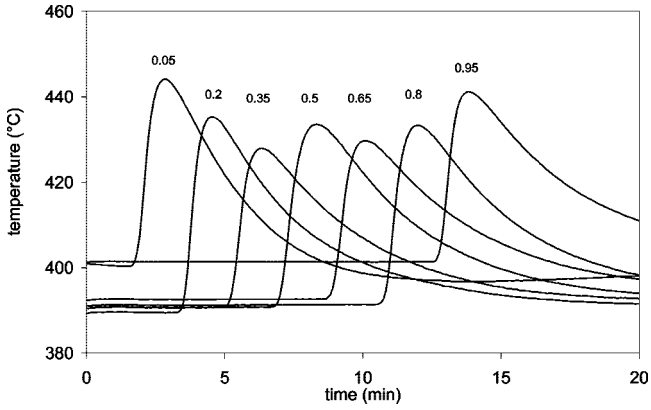

Figure 3. Bed temperatures during adsorption. Parameter: dimensionless axial position *z*/*L*. For reaction conditions refer to Figure 2.

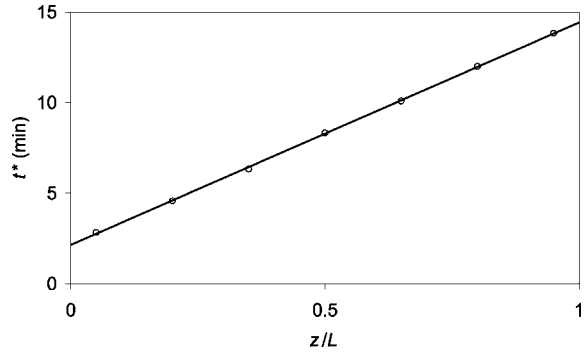

Figure 4. Time since start of feeding to reach maximum temperature as a function of axial position. Reaction conditions as in Figure 2.

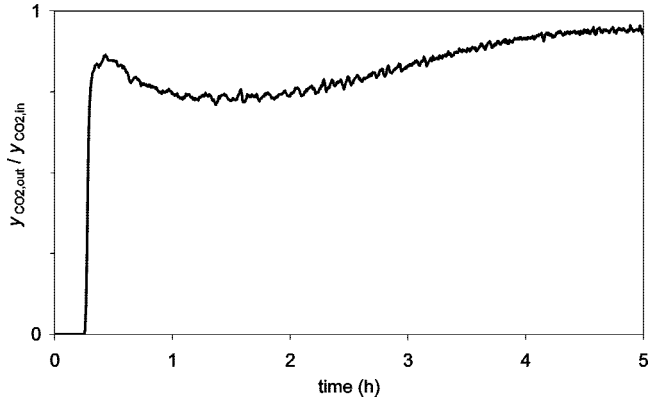

Figure 5. Slow uptake of CO_2 continues for hours after breakthrough. Inlet composition 20% CO_2, 40% H_2O, 40% N_2, total flow 11 slpm, total pressure 28 bar, temperature 400 °C.

of the reactor bed by purging with steam at atmospheric pressure at 400 °C until the effluent dry gas flow was zero. The effluent CO_2 mole fraction in time is displayed in Figure 5. After breakthrough, the CO_2 level increases sharply, then surprisingly drops slightly, before starting to increase again. After five hours the bed has taken up 8 mmol/g and still continues to take up CO_2. This phenomenon can not be attributed to heat effects since after 30 min after breakthrough bed temperatures remain essentially unchanged within 5 °C. We postulate that in addition to fast adsorption there is a much slower process of CO_2 uptake with a considerably higher capacity.

Similar total sorption capacities were established in desorption experiments following extended cyclic adsorption/desorption experiments. After 900 cycles of sorption and desorption, the reactor bed was purged with steam at atmospheric pressure and

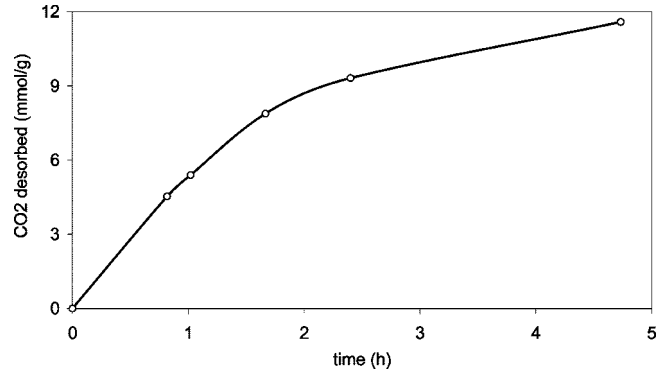

Figure 6. Removal of CO_2 from the sorbent after cyclic tests by purging with 1.8 kg/h steam at atmospheric pressure and 400 °C. A total capacity of CO_2 of 11.6 mmol/g is calculated.

400 °C. After 4.7 h a total quantity of 266 standard liters of dry gas was recovered, which corresponds to a total capacity of at least 11.6 mmol/g (Figure 6). Such high capacity of this material is consistent with an observed uptake of 8.3 mmol/g reported by Allam et al. [5] for a continuous six day exposure under dry conditions as well as for a one day exposure under cyclic, wet conditions. These high capacities are observed in the current research when exposing the sorbent for extended periods at realistic conditions, that is, at high partial pressures of CO_2 and in the presence of steam. The high capacities are not predicted by any of the adsorption isotherms for potassium-promoted hydrotalcite-based materials in literature, which generally predict total capacities on the order of 1−3 mmol/g.[6,16−20] The main difference between this study and those in the literature is the presence of quite substantial amounts of steam and the high CO_2 partial pressure during adsorption. As a consequence, these adsorption isotherms are of limited use when modeling the SEWGS process. Although we do not understand the nature of the slow accumulation process, we have confirmed both the fast and slow uptake process to be reversible. After a full desorption a breakthrough experiment was conducted and a breakthrough capacity similar to previously measured capacities was obtained.

A possible explanation of these observations is the presumption of two reversible sorption processes occurring in series. The first process is fast adsorption and occurs on the sorbent surface. A second process is associated with the slow uptake of CO_2 in the bulk of the active phase of the sorbent. It is interesting to note that were all the Mg in this sorbent transformed into $MgCO_3$, and only Mg species were to take part in the sorption process, a capacity of 9.5 mmol/g would be expected. This is based on information from the manufacturer expressed in terms of an Al_2O_3:MgO:K_2CO_3 ratio. Our findings are consistent with the observations and modeling by Ebner et al.,[16,17] who described the kinetics of CO_2 uptake by a K-promoted hydrotalcite-based material as a coupling of a fast CO_2 chemisorption and two slow conversion reactions supposedly forming carbonates. All three reactions were shown to be completely reversible.

The data of Allam et al.[5] suggests that, under dry conditions, the rate of the slow uptake of CO_2 increases with increasing partial pressure of CO_2 in the gas phase. This may explain why most thermogravimetric experiments, typically operated at 1 bar or less of CO_2, fail to show the same extent of CO_2 capacity as the high pressure runs described here. In the TGA experiments the slow uptake rate is negligible and only the fast adsorption process is observed. This is also likely the case during adsorption isotherm measurements, the extended uptake of CO_2 is generally

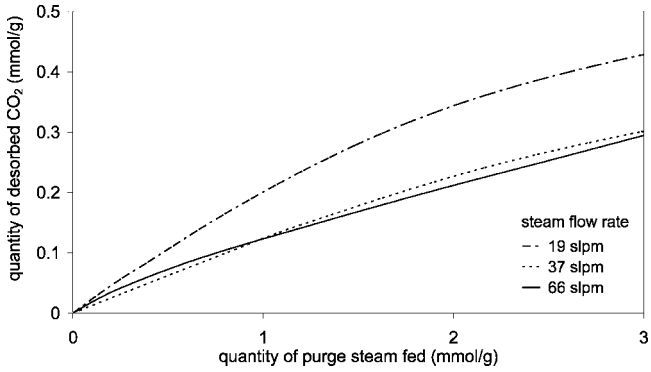

Figure 7. Effect of steam flow rate on desorption rate at 400 °C. Initially the bed was loaded with 2.2 slpm CO_2, 7 slpm N_2, and 1.8 slpm H_2O during 20 min.

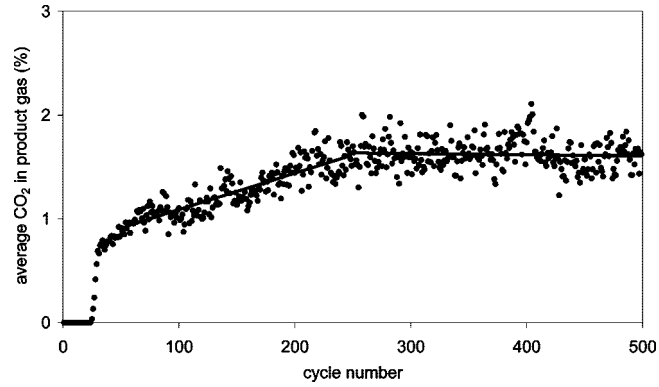

Figure 8. Cycle-averaged CO_2 level of the top product over 500 cycles, showing cyclic stability after 250 cycles. CO_2 rinse cycle. Feed at 400 °C, 28 bar, 20% CO_2, during purge steam-to-CO_2 is 2.2 mol/mol. Working capacity is 0.29 mmol/g.

so slow that it may remain unnoticeable. Since the SEWGS process necessarily requires exposure of the adsorbent to high CO_2 partial pressures, for instance in the feed step, it is important to obtain additional understanding of this slow mechanism of CO_2 removal.

The quantity of steam needed to regenerate the sorbent has a strong impact on the efficiency of the SEWGS-based power plant and on the working capacity of the sorbent. Hence, experiments were conducted to determine the regeneration efficiency at various purge flow rates within the typical industrial range. Each experiment was preceded by a fixed procedure of saturating the sorbent with 20% CO_2, 16% H_2O, balance N_2 at 28 bar for 20 min−some five minutes longer than required for the initial breakthrough of CO_2−followed by a countercurrent reactor depressurization to atmospheric pressure and one complete rinse of the reactor with steam to push out the gas present in the reactor voids. Superheated steam at essentially atmospheric pressure was then fed countercurrently at constant flow rate, and the flow rate of the dry gas leaving the reactor was recorded. Assuming all gas is CO_2, the additional quantity of CO_2 desorbed can be plotted versus the quantity of steam fed. When both quantities are divided by the weight of the sorbent bed, a plot such as Figure 7 is obtained. Those data show that for the lowest purge flow rate the regeneration efficiency is highest, while for the two higher purge flow rates the regeneration efficiencies are similar.

The impact on the SEWGS process is as follows. If a fixed total amount of purge steam per cycle is assumed (2 mmol/g), then the data in Figure 7 indicate that 62% more CO_2 is removed with a steam flow rate of 19 slpm compared to 66 slpm. This means that roughly 62% more feed can be handled every cycle with 19 slpm purge. Since the total amount of steam per cycle is fixed, the SEWGS process using 19 slpm will be more steam efficient, as fewer moles of purge steam are used per mole feed processed. However, the use of 19 slpm steam will also increase the amount of time needed to purge the beds by a factor of $66/19 = 3.5$, which will subsequently increase the overall process cycle time. Higher cycle time means that fewer cycles are completed per day, and the productivity of the process will decrease. More or larger reactor vessels will be needed to process all of the feed gas. Thus, the proper choice of steam purge rate is a balance between steam efficiency and SEWGS capital costs.

CO_2 Cycling. Two important properties of the sorbent associated with feasibility of the SEWGS process are sufficient working capacity: the quantity of CO_2 that is adsorbed and desorbed in one cycle and stability of the sorbent over repeated cycles, that is, stable product purity and recovery. These issues were addressed in extended cyclic experiments in which two different cycles were investigated. In cycle 1 the reactor is cocurrently rinsed with CO_2, whereas in cycle 2 the reactor is countercurrently rinsed with steam. The feed gas consisted of 12% CO_2 in H_2O and N_2 for cycle 1 and 16% CO_2 in H_2O and N_2 for cycle 2. The details of both cycles are listed in Table 1. The cyclic experiments were preceded by complete desorption of CO_2 by countercurrently purging with steam at atmospheric pressure, followed by countercurrently purging with nitrogen at atmospheric pressure for at least 12 h. The same sorbent sample was used for both the CO_2 rinse cycle and the steam rinse cycle, which were performed consecutively in this order.

A first extended experiment was conducted using cycle 1. During the experiments the CO_2 concentration and dry flow rate were recorded, so that the average CO_2 concentration in the reactor effluent gas during the feed step could be calculated. In the first few cycles the first four thermocouples showed exotherms during the feed step, from which it was concluded that adsorption took place in the bottom half of the reactor. However, with increasing cycle number the adsorption front progressed toward the top part of the reactor, as it was observed that the exotherms in the bottom part became less sharp and thermocouples in the top part began to show exotherms as well. Figure 8 shows a plot of the average CO_2 level in the product gas during the feed step versus the cycle number. Three regimes are visible. In the first 25 cycles CO_2 slip is absent. Then suddenly CO_2 slip appears. Here, the adsorption front has just reached the reactor exit at the end of the feed step. The CO_2 level in the top product rises to 1.7% after 250 cycles and then stabilizes at that level until the end of the experiment after 500 cycles. This purity would translate to a CO_2 capture level of 94%. The increasing level of CO_2 in the product gas indicates that the effective working capacity of the sorbent decreases during the first 250 cycles, which is due to an incomplete regeneration and a subsequent CO_2 accumulation on the sorbent. After 250 cycles, the accumulation on the sorbent ends and a so-called cyclic steady state is obtained. The thermocouples in the bed reveal that in this situation reversible adsorption takes place primarily in the second half of the bed. The CO_2 capture level can be easily changed by varying cycle parameters, such as feed time or steam purge quantity. The data in Figure 8 provides important evidence that the observed CO_2 slip in the top product eventually stabilizes and a cyclic steady-state condition can be achieved.

We presume that the accumulation of CO_2 over the first 250 cycles and the appearance of CO_2 in the hydrogen-rich product stream is associated with the CO_2 uptake in the bulk phase of

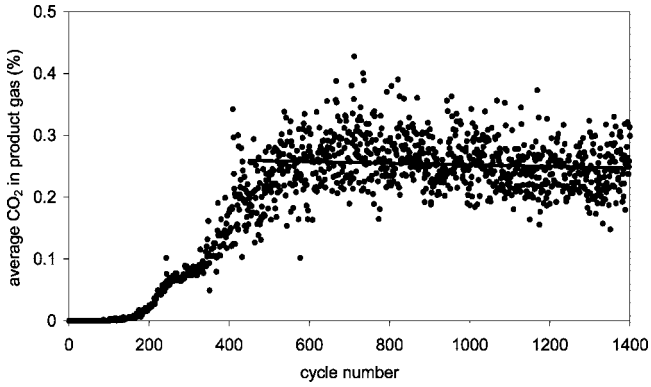

Figure 9. Cycle-averaged CO_2 level of the top product over 1400 cycles, showing cyclic stability after 250 cycles. Steam rinse cycle. Feed at 400 °C, 28 bar, 20% CO_2. Steam-to-CO_2 is 1.9 mol/mol for rinse and 2.5 mol/mol for purge. Working capacity is 0.66 mmol/g.

the sorbent. It is postulated that the accumulation of CO_2 in the bulk phase may retard the fast adsorption process on the sorbent surface, leading to a loss of cyclic capacity. As a consequence, the adsorption front progresses further into the bed and eventually leads to increased CO_2 slip in the hydrogen-rich product stream. Increasing CO_2 slip in this stream was also observed by Allam et al.[5] Future work will focus on clarifying the nature, mechanisms, and interaction of the slow and fast CO_2 uptake on hydrotalcite-based materials.

The results of the previous cyclic experiments led to two important conclusions: (i) the inclusion of a CO_2 rinse step in a SEWGS cycle decreases the working capacity since not only CO_2 from the feed but also large additional amounts of CO_2 during the rinse step need to be reversibly adsorbed per cycle, and (ii) the accumulation of CO_2 in the bulk of the material further reduced the working capacity, and this loss is exacerbated by the presence of CO_2 in the rinse step.

An alternative cycle containing a steam rinse instead of CO_2 rinse was proposed. Steam is an ideal rinse fluid since it can be condensed and easily separated from the desired CO_2. High pressure steam is also available in the power process from the heat recovery and steam generation (HRSG) unit. Preliminary calculations show that additional benefits could be gained with this alternative cycle such as reduction of the number of vessels and valves as well as reduction of vessel sizes, thus reducing SEWGS capital costs by up to 30%.[4]

Extended tests were conducted to verify the feasibility of this cycle 2. High pressure steam corresponding to a steam-to-CO_2 ratio of 1.8 mol/mol was used to effectively displace void gas from the bed. The average CO_2 concentration in the product gas during the feed step is plotted against the cycle number in Figure 9. The level starts to rise gradually after 150 cycles. After 450 cycles the CO_2 level stabilizes at 0.26% for at least another 1000 adsorption and desorption cycles. This purity would translate to a stable CO_2 capture level of 99%, which indicates that CO_2 recoveries well above 90% can be obtained. The stable, cyclic capacity is more than double the working capacity using the cycle with CO_2 rinse. The cyclic capacity in cycle 1 is penalized by the additional sorption of CO_2 during the rinse step. The higher capacity in cycle 2 will result in smaller vessel sizes and lower capital costs, along with improved efficiency for CO_2 capture due to reduced rinse gas requirements.

After the cyclic experiment the sorbent was cleaned with steam and in a following breakthrough experiment the breakthrough capacity was determined to be similar to previously measured capacities. Thus, the sorbent is stable after the extended cyclic testing.

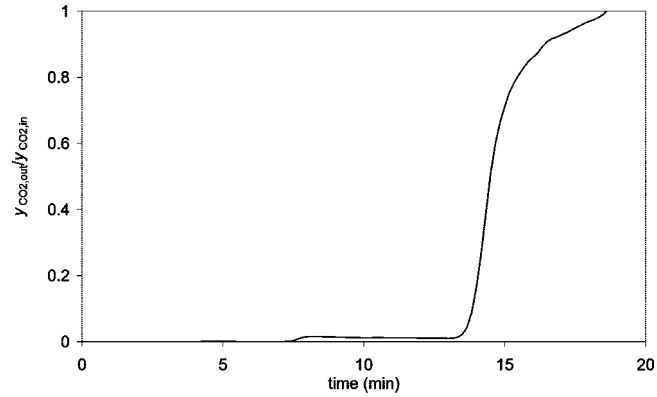

Figure 10. Breakthrough curve for CO_2. Breakthrough capacity is 1.35 mmol/g. CO_2, 2 slpm; N_2, 7 slpm; H_2O, 3 slpm; 28 bar; 400 °C.

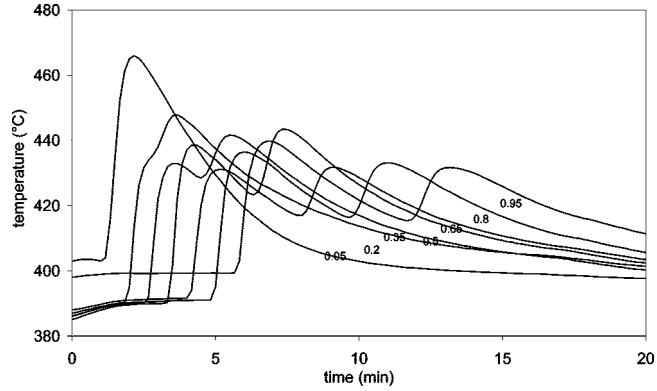

Figure 11. Bed temperatures during adsorption. Parameter: dimensionless axial position.

3.2. Sorption-Enhanced Reaction Experiments. For subsequent experiments the sorbent material was mixed with pellets of iron−chromium shift catalyst and loaded into the reactor. A first experiment was aimed at confirming the breakthrough capacity of the sorbent, which came from the same batch of K-promoted hydrotalcite-based material used in the first series of experiments. The bed was then exposed to a mixture of CO_2, CO, H_2O, H_2, and N_2 to assess the reaction enhancement by sorption as well as determine the stability of the sorbent and catalyst under extended cyclic conditions.

CO_2 Breakthrough in the Presence of Catalyst. The first experiment with the new reactor loading was a CO_2 breakthrough experiment to verify the breakthrough capacity. Figure 10 shows the CO_2 level of the effluent when feeding a mixture of 18% CO_2, 25% H_2O, and balance N_2 at 400 °C and 28 bar. After 7 min a small CO_2 slip is observed: the effluent contains about 0.3% CO_2. Breakthrough of CO_2 occurs 13 min after starting the feed. The breakthrough capacity is 1.35 mmol/g, which is similar to the capacity established in the first series of experiments (1.4 mmol/g). The shape of the breakthrough curve is also similar to the curve shown in Figure 2.

As Figure 11 shows, the thermocouples in the reactor registered two exotherms during the breakthrough experiment: the first exotherm is slightly larger than the second exotherm. For the thermocouple closest to the inlet both exotherms coincide but further into the bed the two exotherms are separated. The first exotherm is attributed to partial reoxidation of the catalyst by steam and the second exotherm is attributed to the CO_2 adsorption. Oxidation of Fe_3O_4 to Fe_2O_3 is calculated to be nearly thermoneutral at a temperature of 400 °C. It is therefore assumed that oxidation of over-reduced catalyst FeO to Fe_3O_4 ($\Delta_r H = -104$ kJ/mol$_{Fe}$) occurs. Presumably steam starts to break

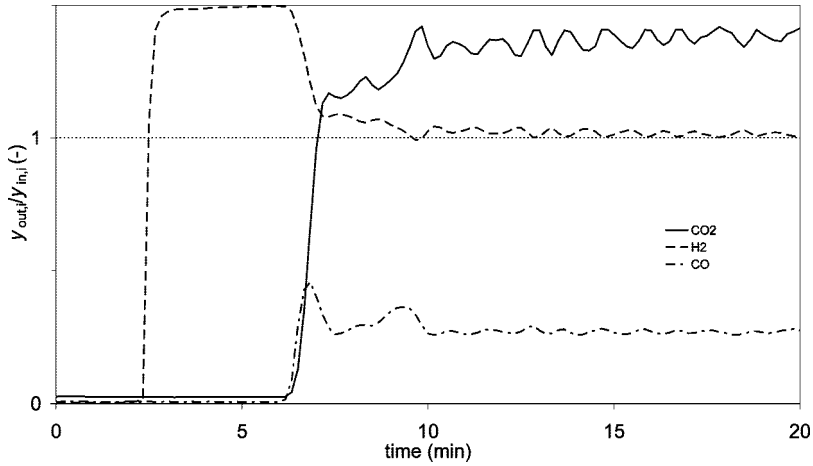

Figure 12. Breakthrough curve for CO_2 and CO. CO and CO_2 break through simultaneously. Molar fractions y_i are dry basis. $CO_2/CO/H_2/H_2O$ = 3.2/1.9/11.2/3.1 slpm; 28 bar.

through 7 min after start of the feed. Because of the oxidation the bed temperature has risen over 40 °C, which could cause some carbonates to be dissociated to CO_2 that ends up in the effluent. This is consistent with the observation of a small but decreasing CO_2 slip after 7 min, as shown in Figure 10. The second exotherm is associated with the adsorption of CO_2. This thermal front passes the last thermocouple 13 min after the start of the experiment, just before breakthrough of CO_2 begins. All temperatures drop to their initial values after prolonged exposure. Subsequent breakthrough experiments yielded much smaller exotherms for the oxidation reaction, viz., 10 °C, but otherwise similar results.

Sorption-Enhanced Reaction. In a following experiment it was demonstrated that CO conversion can be enhanced to 100% in the presence of a CO_2 sorbent. Before starting the experiment CO_2 was desorbed from the sorbent by purging the reactor countercurrently with steam at atmospheric pressure until dry gas flow in the effluent was essentially zero. Then the reactor was countercurrently pressurized to 28 bar using N_2. The experiment started by feeding a gas mixture (58% H_2, 16% CO_2, 10% CO, 16% H_2O) at 400 °C and 28 bar to the reactor. The composition was comparable to the feed of a SEWGS unit, and the chemical equilibrium temperature of the gas mixture was 472 °C. The effluent composition was measured, and the measured concentrations normalized by the inlet concentrations are plotted for all components except H_2O in Figure 12. These data show that all of the N_2 is initially purged from the reactor voids and then after 2 min a nearly pure H_2 stream breaks through. At this point, CO in the feed gas is converted to CO_2 and all of the CO_2 is taken up by the sorbent. Without the sorbent, conversion would be thermodynamically limited. Indeed, this is a strong indication that sorption can enhance the shift reaction under realistic SEWGS conditions. As such, y_{out,H_2} becomes 1 and thus $y_{out,H_2}/y_{in,H_2}$ is 1.46 (dry basis). CO_2 breakthrough occurs 6 min after starting the feed, yielding a consistent breakthrough capacity of 1.4 mmol/g. At breakthrough, CO and CO_2 simultaneously appear at the product end of the bed. It can be deduced from the sharp CO_2 breakthrough curve that a sufficient amount of catalyst is present in the reactor, otherwise small amounts of CO would slip through before the CO_2 adsorption front has reached the reactor outlet. After breakthrough of CO_2 and CO, CO is still partially converted, as can be expected since the feed gas composition is not at chemical equilibrium at a reactor temperature of 400 °C.

In Figure 13, the bed temperatures during the sorption-enhanced reaction are presented. The exotherms are slightly

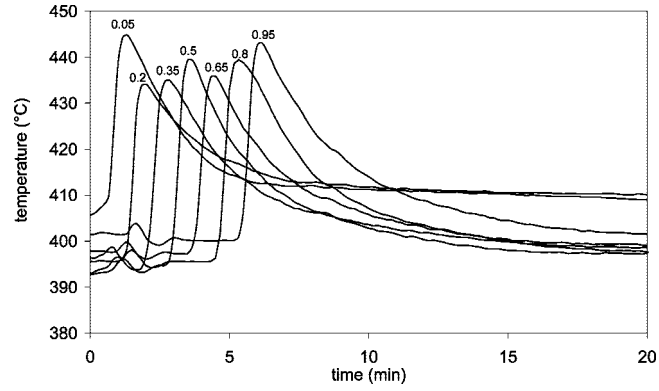

Figure 13. Bed temperatures during adsorption and reaction. Parameter: dimensionless axial position. For conditions see Figure 10.

higher than those observed for the adsorbent-only experiments (cf. Figure 3). Of course, the exothermal shift reaction ($\Delta_r H$ = −38.2 kJ/mol at 400 °C) adds to heat generated by CO_2 adsorption. Additionally, it should be noted that the first two thermocouples, at z/L = 0.05 and 0.2, do not fall back to their initial values. Hence, the temperature in the first part of the reactor remains higher than the inlet gas temperature because of the heat generated by the shift reaction, which continues after breakthrough. This indicates that the feed gas is not at its thermochemical equilibrium at the inlet temperature of the bed and reacts toward a new equilibrium state. Under these conditions, methane formation as a side reaction on this high-temperature catalyst was negligible, since the level of methane in the effluent was measured at 7 ppm.

SEWGS Cycling. In a following series of experiments the stability of the sorbent and catalyst under extended cyclic conditions was investigated.

In the first experiment the CO_2 rinse cycle, denoted as cycle 3 in Table 1, was applied. The CO and CO_2 levels of the H_2 product gas during the feed step are plotted against cycle number in Figure 14. During 185 cycles of adsorption/reaction and desorption the purity of the H_2 product stream and CO conversion are confirmed to be stable. At cycle 185 the amount of purge steam was reduced so the molar steam-to-CO_2 ratio is decreased from 3.3 to 2.2. The CO_2 and CO level in the H_2-rich product gas started to climb, but even after 150 cycles under these new conditions the level of impurities remain below 300 ppm. The quantity of CO_2 in the product gas was roughly 17 times the quantity of CO.

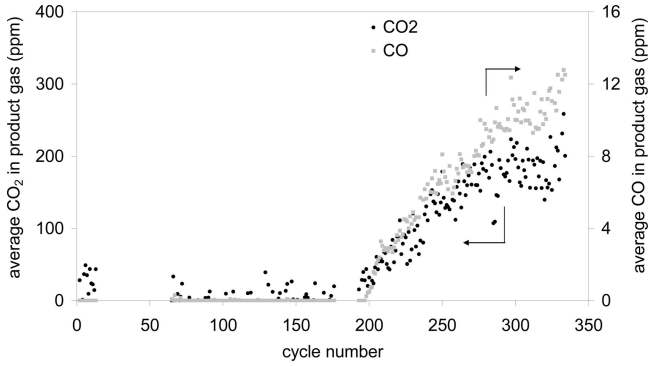

Figure 14. Cycle-averaged CO_2 and CO levels of the H_2 product during the feed step over 335 cycles. CO_2 rinse cycle. Feed at 400 °C, 28 bar, 12% CO_2, 1.6% CO, during purge steam-to-C is 3.3 mol/mol up to cycle 185 and 2.2 mol/mol onward. During cycles 14−64 and 177−192 no measurements of the top product were taken.

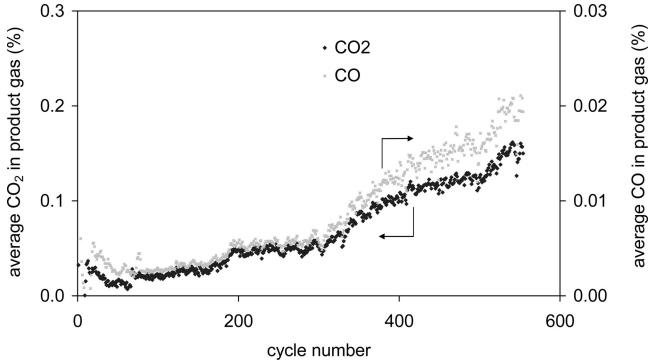

Figure 15. Cycle-averaged CO_2 and CO levels of the top product during the feed step over 550 cycles. Steam rinse cycle. Feed at 400 °C, 28 bar, 12% CO_2, 1.6% CO, 21% H_2O. Steam-to-C is 2.3 mol/mol for rinse and 2.3 mol/mol for purge. Feed flow: CO_2, 2.2 slpm; N_2, 7 slpm; H_2O, 3 slpm; 28 bar; 400 °C.

A similar experiment was undertaken to investigate the performance using a steam rinse cycle, denoted by cycle 4 in Table 1. The CO and CO_2 levels of the H_2-rich product stream during the feed step are plotted against cycle number in Figure 15. Low levels of CO_2 and CO appear essentially from the start and increase slightly but after 550 cycles CO_2 level is still below 0.15% and CO level is still below 0.02%. This would correspond to a CO_2 recovery of 99.3% and a CO conversion of 99.2%. The quantity of CO_2 in the product gas equals eight times the quantity of CO; this is confirmed to correspond to chemical equilibrium at 400 °C.

After completion of the extended cyclic tests the methane formation was again investigated. A CH_4 level of 175 ppm in the effluent was measured, noticeably larger than before experiments started, but still CH_4 formation is small and quite acceptable. The small methanation activity could possibly be caused by overreduction of the catalyst predominantly at the top of the bed, due to the presence of reducing conditions during the feed step.

4. Conclusions

The sorption-enhanced water−gas shift (SEWGS) process is a novel route for precombustion decarbonization. The process exploits the synergy of CO_2 removal by adsorption and CO conversion at elevated temperatures and pressures. In a dedicated, 2 m tall packed-bed reactor the characteristics of a K-promoted hydrotalcite-based sorbent were investigated. Under realistic SEWGS feed conditions, the typical breakthrough capacity of this material is 1.4 mmol/g. The existence of a sharp adsorption front was confirmed by the observed breakthrough curves and the well-defined exotherms in the bed. After breakthrough CO_2 continues to be taken up by the bed albeit at a much lower rate. It was shown that the total capacity of this material can exceed 10 mmol/g. This large capacity is associated with a slow CO_2 uptake mechanism, while the breakthrough capacity is associated with a much faster adsorption mechanism. Both processes appear to be completely reversible. During cyclic operation for more than 1400 adsorption and desorption cycles, the CO_2 slip through the sorbent bed is very low and remains stable. Carbon recoveries well above 90% can be obtained. The sorbent shows a stable working capacity. In this cycle, a total amount of 4.4 moles of steam per mole of CO_2 is applied for the rinsing and purging steps. Further reduction of steam demand is expected to be feasible by process and cycle optimization and by allowing slightly higher CO_2 slip.

The SEWGS process concept was demonstrated in a reactor packed with a mixture of a potassium-promoted hydrotalcite-based sorbent and a commercial iron−chromium shift catalyst. CO conversion was enhanced to 100% in the presence of a CO_2 sorbent until breakthrough of CO_2. At breakthrough, CO and CO_2 simultaneously appear in the product gas. The CO_2 capture rate and CO conversion were confirmed to be stable for more than 300 cycles of adsorption/reaction and desorption, applying 4.6 moles steam per mole CO_2. These experimental results will allow optimization of process conditions and cycle parameters for scale-up to a pilot unit, which will demonstrate precombustion decarbonization in natural-gas based power generation or hydrogen production.

Acknowledgment

Support from the European Commission (Contract No. 019972) and CCP-2 is gratefully acknowledged. The authors would like to thank the Cachet work package technical team for their valuable suggestions.

Literature Cited

(1) IPCC. Summary for Policymakers. In *Climate Change 2007: The Physical Science Basis;* Contribution of Working Group I to the Fourth Assessment Report of the Intergovernmental Panel on Climate Change; Solomon, S., Quin, D., Manning, M., Chen, Z., Marquis, M., Averyt, K. B., Tignor, M., Miller, H. L., Eds.; Cambridge University Press: Cambridge, U.K., and New York, 2007.

(2) IPCC. Summary for Policymakers. In *Climate Change 2007: Mitigation*; Contribution of Working Group III to the Fourth Assessment Report of the Intergovernmental Panel on Climate Change; Metz, B., Davidson, O. R., Bosch, P. R., Dave, R., Meyer, L. A., Eds.; Cambridge University Press: Cambridge, U.K., New York, 2007.

(3) Hufton, J. R.; Allam, R. J.; Chiang, R.; Middleton, P.; Weist, E. L.; White, V. *Development of a Process for CO_2 Capture from Gas Turbines Using a Sorption Enhanced Water Gas Shift Reactor System*; Proceedings of the 7th International Conference on Greenhouse Gas Technology; Vancouver, Canada, 2004.

(4) Allam, R. J.; Chiang, R.; Hufton, J. R.; Middleton, P.; Weist, E. L.; White, V. Development of the Sorption Enhanced Water Gas Shift Process. In *Carbon Dioxide Capture for Storage in Deep Geologic Formations*; Thomas, D. C., Benson, S. M., Eds.; Elsevier Ltd.: Oxford, 2005; Vol 1, pp 227−256.

(5) Allam, R. J.; Hufton, J. R.; Quinn, B.; White, V. *Production of Hydrogen Fuel by Sorbent Enhanced Water Gas Shift Reaction.* DOE−Air Products Cooperative Agreement, Final Report, 2005.

(6) Cobden, P. D.; van Beurden, P.; Reijers, H. Th. J.; Elzinga, G. D.; Kluiters, S. C. A.; Dijkstra, J. W.; Jansen, D.; van den Brink, R. W. Sorption-Enhanced Hydrogen Production for Pre-combustion CO_2 Capture: Thermodynamic Analysis and Experimental Results. *Int. J. Greenhouse Gas Control* **2007**, *1*, 170–179.

(7) Hufton, J. R.; Mayorga, S.; Sircar, S. Sorption-Enhanced Reaction Process for Hydrogen Production. *AIChE J.* **1999**, *45*, 248.

(8) Yong, Z.; Mata, V.; Rodrigues, A. E. Adsorption of Carbon Dioxide at High Temperature—A Review. *Sep. Purif. Technol.* **2002**, *26*, 195–205.

(9) Hufton, J. R.; Weigel, S. J.; Waldron, W. F.; Rao, M. B.; Nataraj, S.; Sircar, S.; Gaffney, T. R. *Sorption Enhanced Reaction Process for Production of Hydrogen*. DOE−Air Products Cooperative Agreement #DE-FC36-95G010059, Final Report, 2000.

(10) Ding, Y.; Alpay, E. Adsorption-Enhanced Steam-Methane-Reforming. *Chem. Eng. Sci.* **2000**, *55*, 3461–3474.

(11) Ding, Y.; Alpay, E. Equilibria and Kinetics of CO_2 Adsorption on Hydrotalcite Adsorbent. *Chem. Eng. Sci.* **2000**, *55*, 3929–3940.

(12) Yong, Z.; Rodrigues, A. E. Hydrotalcite-like Compounds as Adsorbents for Carbon Dioxide. *Energy Conv. Manage.* **2002**, *43*, 1865–1876.

(13) Reijers, H. Th. J. ; Roskam-Bakker, D. F.; Dijkstra, J. W.; Smit, R.; de Groot, A.; van den Brink, R. W. *Hydrogen Production Through Sorption-Enhanced Reforming*; Proceedings of the 1st European Hydrogen Energy Conference, Grenoble, France, September 2−5, 2003.

(14) Reijers, H. Th. J.; Valster-Schiermeier, S. E. A.; Cobden, P. D.; van den Brink, R. W. Hydrotalcite as CO_2 Sorbent for Sorption-Enhanced Steam Reforming of Methane. *Ind. Eng. Chem. Res.* **2006**, *45*, 2522–2530.

(15) Moreira, R. F. P. M.; Soares, J. L.; Casarin, G. L.; Rondrigues, A. E. Adsorption of CO_2 on Hydrotalcite-like Compounds in a Fixed Bed. *Sep. Sci. Technol.* **2006**, *41*, 341–357.

(16) Ebner, A. D.; Reynolds, S. P.; Ritter, J. A. Understanding the Adsorption and Desorption Behavior of CO_2 on a K-Promoted Hydrotalcite-like Compound (HTlc) through Nonequilibrium Dynamic Isotherms. *Ind. Eng. Chem. Res.* **2006**, *45*, 6387–6392.

(17) Ebner, A. D.; Reynolds, S. P.; Ritter, J. A. Non-Equilibrium Kinetic Model that Describes the Reversible Adsorption and Desorption Behavior of CO_2 in a K-Promoted HTlc. *Ind. Eng. Chem. Res.* **2007**, *46*, 1737–1744.

(18) Lee, K. B.; Beaver, M. G.; Caram, H. S.; Sircar, S. Reversible Chemisorption of Carbon Dioxide: Simultaneous Production of Fuel-Cell Grade H_2 and Compressed CO_2 from Synthesis Gas. *Adsorption* **2007**, *13*, 385–397.

(19) Lee, K. B.; Beaver, M. G.; Caram, H. S.; Sircar, S. Novel Thermal-Swing Sorption-Enhanced Reaction Process Concept for Hydrogen Production by Low-Temperature Steam-Methane Reforming. *Ind. Eng. Chem. Res.* **2007**, *46*, 5003–5014.

(20) Lee, K. B.; Verdooren, A.; Caram, H. S.; Sircar, S. Chemisorption of Carbon Dioxide on Potassium-Carbonate-Promoted Hydrotalcite. *J. Colloid Interface Sci.* **2007**, *308*, 30–39.

(21) Oliveira, E. L. G.; Grande, C. A.; Rodrigues, A. E. CO_2 Sorption on Hydrotalcite and Alkali-Modified (K and Cs) Hydrotalcites at High Temperature. *Sep. Purif. Technol.* **2008**, *62*, 137.

(22) Walspurger, S.; Boels, L.; Cobden, P. D.; Elzinga, G. D.; Haije, W. G.; van den Brink, R. W. The Crucial Role of the K^+-Aluminium Oxide Interaction in K^+-Promoted Alumina- and Hydrotalcite-Based Materials for CO_2 Sorption at High Temperatures. *ChemSusChem* **2008**, *1*, 643–650.

(23) Ram Reddy, M. K.; Xu, Z. P.; Lu, G. Q.; Diniz da Costa, J. C. Influence of Water on High Temperature CO_2 Capture Using Layered Double Hydroxide Derivatives. *Ind. Eng. Chem. Res.* **2008**, *47*, 2630–2635.

(24) Anand, M.; Hufton, J.; Mayorga, S.; Nataraj, S.; Sircar, S.; Gaffney, T. Sorption Enhanced Reaction Process (SERP). *Proc. U.S. DoE Hydrogen Program Rev.* **1996**, 537–549.

(25) Reynolds, S. P.; Ebner, A. D.; Ritter, J. A. New Pressure Swing Adsorption Cycles for Carbon Dioxide Sequestration. *Adsorption* **2005**, *11*, 531–536.

(26) Reynolds, S. P.; Ebner, A. D.; Ritter, J. A. Stripping PSA Cycles for CO_2 Recovery from Flue Gas at High Temperature Using a Hydrotalcite-like Adsorbent. *Ind. Eng. Chem. Res.* **2006**, *45*, 4278–4294.

Received for review November 11, 2008
Revised manuscript received February 17, 2009
Accepted February 17, 2009

IE801713A